Return of your e-proof to AMS via the task assigned to you in Editorial Manager signifies:

*** You have thoroughly read the proof and authorize publication (except where you have identified errors or indicated changes within the proof file or a text file summarizing the changes)**

***You agree to pay all publication charges (except for WCAS and cases where a waiver has been previously granted)**

***You understand that adjustments for AMS style may be made prior to publication.**

Proofreading
To correct the page proofs and return them to AMS, electronically annotate the PDF file containing your proof using **the annotation and commenting tools (NOT the editing tools)** in Adobe Acrobat as described below and submit the annotated PDF via the Editorial Manager journal site following the instructions provided in the task assignment email sent to you.

We request that you return the annotated proof within two business days of downloading it in order to facilitate final publication as quickly as possible. Note that this response time is strongly encouraged, but not required.
Proofread the proofs carefully, as this will be your only chance to see your article before publication. Pay special attention to color figures (if any), Greek letters, and mathematical symbols.

If your paper contains supplemental material, please note the hyperlink will not be active in the proof. The link will be activated upon publication of your article.

Alterations
In addition to page charges, additional charges may be assessed for excessive changes/edits to typeset proofs and for the processing of multiple figure files for single figures.

Please see the Frequently Asked Proof Editing Questions page for commonly requested changes and points of AMS style (www.ametsoc.org/PubsProofEditingFAQs).

The proof contains keywords that correspond to the classifications chosen during manuscript submission in Editorial Manager. These keywords will appear in the published article. If a keyword needs to be changed you can note that within the proof, but only keywords included in the existing list of available terms on our website can be used (www.ametsoc.org/PubsKeywords). Terms that do not appear in this list cannot be used for your article keywords. If you have a suggestion for a new term that should be considered for addition to the list when the taxonomy is periodically reviewed and updated, please contact PubsKeywords@ametsoc.org.

The layout in the page proof is considered final unless changes are essential. Please also note that material changes to the *scientific content* of the manuscript at this stage will require further peer review, substantially increasing the time to publication. **The editors reserve the right to accept or reject proposed alterations.** If there are significant changes and the editor determines that a full revised proof needs to be generated it may be sent to you to check.

Figures
The figures that appear in your page proofs are lower resolution than the final printed article. The primary AMS technical editor for your journal will be reviewing figure quality prior to publication. If you have specific concerns about any of your figures, especially if any color figures do not appear in color, please describe them in your comments. Please verify that each figure properly corresponds with the figure captions and citations in the text. If there are figure corrections that need to be made, upload a new electronic version of the corrected figure with your corrected proofs.

Thank you very much for your cooperation and thank you for publishing with AMS. For questions or more information, please contact authorproofs@ametsoc.org.

Annotating PDFs using Adobe Acrobat Reader DC

Please note before you begin:
A. While working on your proof, it is important to use only the Commenting/annotation tools. Please do NOT use editing tools.
B. The commenting tools and toolbars in older versions of Acrobat and Reader will look different, but they will still operate the same as tools shown below. If you are using an older version, we recommend an update to Adobe Acrobat Reader DC, which can be downloaded and installed for free - please see step 1 below for more information.

1. Update to Adobe Acrobat Reader DC
The screen images in this document were captured on a Windows PC running Adobe Acrobat Reader DC. Upgrading to the newest version is not always necessary, but it is preferable, and these instructions apply *only* to Adobe Acrobat Reader DC. You can also create annotations using any version of Adobe Acrobat. Adobe Acrobat Reader DC can be downloaded at no cost from http://get.adobe.com/reader/

2. What are eProofs?
eProof files are self-contained PDF documents for viewing on-screen and for printing. They contain all appropriate formatting and fonts to ensure correct rendering on-screen and when printing hardcopy. SJS sends eProofs that can be viewed, annotated, and printed using either Adobe Acrobat Reader or Adobe Acrobat.

3. Show the Comment Toolbar

4. Using the PDF Comments menu
To *insert new text,* place your cursor where you would like to insert the new text, and type the desired text. To *replace* text, highlight the text you would like to replace, and type the desired replacement text. To *delete* text, highlight the text you would like to delete and press the Delete key.

Acrobat and Reader will display a pop-up note based on the modification (e.g., inserted text, replacement text, etc.). To format text in pop-up notes, highlight the text, right click, select Text Style, and then choose a style. A pop-up note can be minimized by selecting the X button inside it. When inserting or replacing text, a symbol indicates where your comment was inserted, and the comment is shown in the Comments List. **If you do not see the comments list, you are editing the live text instead of adding comments, and your changes are not being tracked. Please make certain to use the Comments feature instead.**

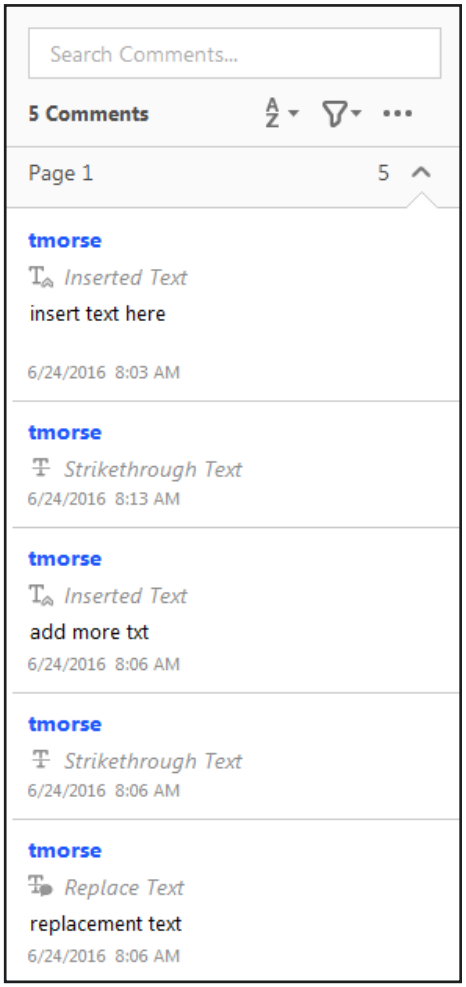

5. Inserting symbols or special characters
An insert symbol feature is not available for annotations, and copying/pasting symbols or non-keyboard characters from Microsoft Word does not always work. Use angle brackets < > to indicate these special characters (e.g., <alpha>, <beta>).

6. Editing near watermarks and hyperlinked text
eProof documents often contain watermarks and hyperlinked text. Selecting characters near these items can be difficult using the mouse. To edit an eProof which contains text in these areas, do the following:

- Without selecting the watermark or hyperlink, place the cursor near the area for editing.
- Use the arrow keys to move the cursor beside the text to be edited.
- Hold down the shift key while simultaneously using arrow keys to select the block of text, if necessary.
- Insert, replace, or delete text, as needed.

... continues on page 2

7. Reviewing changes

To review all changes, open the Comment menu and the Comment List is displayed.

Note: *Selecting a correction in the list highlights the corresponding item in the document, and vice versa.*

8. Still have questions?

Try viewing our brief training video at https://authorcenter.dartmouthjournals.com/Article/PdfAnnotation

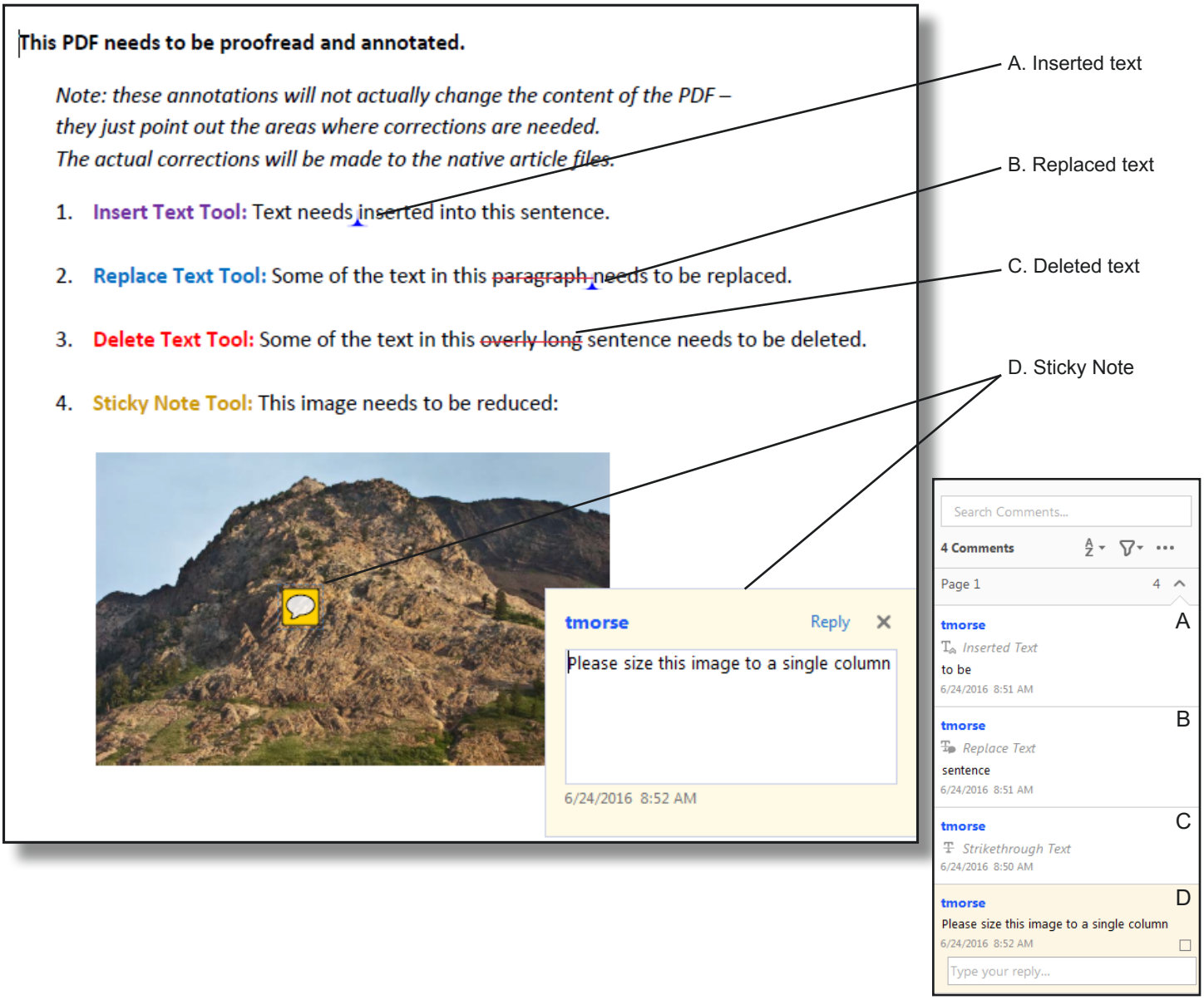

NUMBER 1 OF 1

AUTHOR QUERIES

DATE 10/23/2021
JOB NAME JHM
JOB NUMBER 0

ARTICLE jhmD210083
QUERIES FOR AUTHORS NICHOLSON ET AL.

PLEASE ANSWER THE AUTHOR QUERIES WHERE THEY APPEAR IN THE TEXT.

AU1: The keywords here are the classifications you chose during the manuscript submission process. If you want to add others or replace any of these keywords, please note that only keywords from the predefined list may be used. See http://ametsoc.org/PubsKeywords for more information.
AU2: Part II was not cited, but there was a citation here for Nicholson et al. (2021b), so Part II has been added to the reference list as Nicholson et al. (2021b), and the Nicholson et al. (2021) reference and citations have been changed to (2021a). If this is not correct, please make corrections as necessary and add a citation for Part II where appropriate.

JOBNAME: JHM 00#00 2021 PAGE: 1 SESS: 8 OUTPUT: Sat Oct 23 07:29:54 2021 Total No. of Pages: 11
/ams/jhm/0/jhmD210083

On the Diurnal Cycle of Rainfall and Convection over Lake Victoria and Its Catchment. Part I: Rainfall and Mesoscale Convective Systems

SHARON E. NICHOLSON,[a] ADAM T. HARTMAN,[a] AND DOUGLAS A. KLOTTER[a]

[a] *Department of Earth, Ocean, and Atmospheric Science, Florida State University, Tallahassee, Florida*

(Manuscript received 22 April 2021, in final form 14 September 2021)

ABSTRACT: This article examines the diurnal cycle of lake-effect rains over Lake Victoria and of rainfall in the surrounding catchment. The analysis focuses on four months, which represent the two wet seasons (April and November) and the two dry seasons (February and July). Lake-effect rains are strongest in April and weakest in July. In all cases there is a nocturnal rainfall maximum over the lake and a daytime maximum over the catchment, with the transition between rainfall over the lake and over the catchment occurring between 1200 and 1500 local standard time (LST). During the night the surrounding catchment is mostly dry. Conversely, little to no rain falls over the lake during the afternoon and early evening. In most cases the maximum over the lake occurs at either 0600 or 0900 LST and the maximum over the catchment occurs around 1500–1800 LST. The diurnal cycle of mesoscale convective systems (MCSs) parallels that of overlake rainfall. MCS initiation generally begins over the catchment around 1500 LST and increases at 1800 LST. MCS initiation over the lake begins around 0300 LST and continues until 1200 LST. While some MCSs originate over the highlands to the east of the lake, most originate in situ over the lake. Maximum MCS activity over the lake occurs at 0600 LST and is associated with the systems that initiate in situ.

SIGNIFICANCE STATEMENT: This article presents two new conclusions about rainfall over Lake Victoria. One is that rainfall is enhanced over the lake in all months, even during the dry seasons. The other is that most nocturnal mesoscale systems actually develop in situ over the lake. The results enhance our understanding of the Lake Victoria system, which helps to sustain some 30 million people in East Africa and some 300 million living in the Nile basin. With the threat of climate change looming large, increased knowledge of the lake system will allow for improved estimation of its impact.

AU1 KEYWORDS: Africa; Lake effects; Precipitation; Mesoscale systems

1. Introduction

Lake Victoria, with a surface area of 68 870 km^2, is the world's third largest lake by area (Fig. 1). It provides the livelihood of 30 million people in Kenya, Uganda, and Tanzania. It sustains the fishing industry and agriculture, and it also provides hydroelectric power (Chamberlain et al. 2014). Equally important, Lake Victoria is the source of the White Nile, the life-blood of Sudan, South Sudan, and Egypt. A 1-m rise of Lake Victoria can increase flow throughout the White Nile system by 70%–80% (Sene 2000). Such a rise occurred in 1961, a year in which overlake rainfall reached roughly 2500 mm, or some 50% above the long-term mean (Yin and Nicholson 2002). Between 1998 and 2020 its levels have fluctuated over a range of 3.5 m, creating tremendous variability in the Nile flow.

Over 80% of the input to Lake Victoria is provided by rainfall falling over the lake itself. Regional topography and lake–land breezes (Lumb 1970) enhance overlake rainfall compared to rainfall in the surrounding catchment, with published estimates varying from 28% to 85% (Yin and Nicholson 1998; Kizza et al. 2012; Thiery et al. 2015). The enhancement is apparent in every month, with the ratio of overlake rainfall to catchment rainfall varying between 1.2 and 1.6 (Nicholson et al. 2021a). Significant rainfall occurs over the lake even in months when catchment rainfall averages only 30–40 mm. Annually, the average enhancement was found to be 43%. This value compares favorably with estimates based on rainfall stations both over the catchment and on islands in the lake (e.g., Flohn 1983; Flohn and Burkhardt 1985).

Studies have shown that this region is particularly sensitive to climatic change, so that the longer-term response of the lakes to global warming is a serious concern (Akurut et al. 2014; di Baldassarre et al. 2011). A thorough understanding of the lake-effect rains is critical in evaluating this response and in projecting future water resources.

In this paper, we advance that understanding by evaluating the diurnal cycle of rainfall over the lake and its catchment during wet and dry seasons, by contrasting conditions over the eastern and western portions of the catchment, and by examining the diurnal cycle and spatial distribution of mesoscale convective systems (MCSs) over the lake and surrounding regions. The contribution of MCSs to the diurnal cycle is also investigated. Section 2 reviews prior studies of the diurnal cycle over Lake Victoria. Section 3 describes the methodology and the data utilized. Section 4 shows the diurnal cycle of rainfall. The cycle of MCS activity and initiation is depicted in section 5. A summary and conclusions are presented in section 6.

2. Background

The enhancement of rainfall over Lake Victoria and the nocturnal rainfall maximum have long been known.

Corresponding author: Sharon E. Nicholson, snicholson@fsu.edu

DOI: 10.1175/JHM-D-21-0083.1

JOBNAME: JHM 00#00 2021 PAGE: 2 SESS: 8 OUTPUT: Sat Oct 23 07:29:54 2021 Total No. of Pages: 11
/ams/jhm/0/jhmD210083

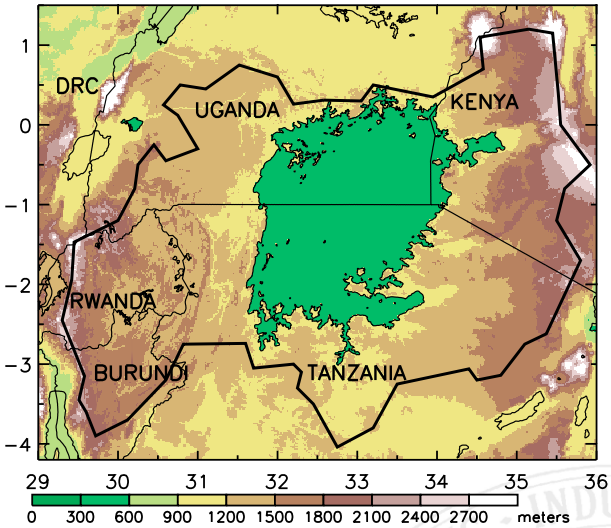

FIG. 1. Image of Lake Victoria and surrounding topography. The solid black line shows the lake catchment.

The lake–land breeze system which controls the rainfall was first detected in 1908 by the Berson (1910) expedition. Further discussion was found in several papers in a compilation by Bargman (1960). Flohn and Fraedrich (1966) and Fraedrich (1968) provided detailed descriptions of the circulation and overlake rainfall based on extensive observations. Fraedrich (1971, 1972) later published a model of the dynamics and energetics of the nocturnal circulation. Kayiranga (1991), Ba and Nicholson (1998), and Yin and Nicholson (1998) focused on convection and rainfall enhancement over the lake, using satellite estimates of cold-cloud duration. Yin et al. (2000) and Nicholson and Yin (2002) described the diurnal cycle of rainfall, evaporation, and cloudiness over Lake Victoria. They confirmed the nocturnal rainfall maximum over most of the lake but found that a late afternoon maximum prevailed in the east, consistent with that over land. Those results were consistent with data from rain gauges over land or islands.

With the improvement of satellite methods for rainfall and lightning assessment, interest in the diurnal cycle over Lake Victoria has reemerged within the last few years. Holle and Murphy (2017) showed intense lightning activity over the lake from 0300 to 1100 local standard time (LST), with maximum activity from 0700 to 1000 LST. Virts and Goodman (2020) found a daytime lightning maximum north and east of the lake, with the nighttime maximum propagating southwestward across the lake. Annually, 85% of lightning clusters that produce over 1000 flashes over the lake initiate in situ, but the most extreme clusters tend to form over land and move over the lake. Initiation is most frequent between 2200 and 0400 LST during the rainy seasons, but between 0500 and 0800 during the two dry seasons. Thiery et al. (2016) got comparable results when evaluating thunderstorm occurrence, using the method of overshooting tops (OTs; Bedka et al. 2010). The method identifies extreme updrafts associated with severe storms. On average the nighttime OTs were concentrated over the western portion of the lake and were completely absent over the catchment. Daytime OTs showed a maximum to the northeast of the lake, coincident with the lightning maximum shown by Virts and Goodman (2020).

Haile et al. (2013) looked at the diurnal cycle of rainfall frequency and intensity in the month of April. Examining the rainfall stations used by Datta (1981) and comparing them with Tropical Rainfall Measuring Mission (TRMM) 3B42 data, they likewise found a daytime maximum in the east and a nighttime maximum in the west. Dezfuli et al. (2017) showed that the daytime maximum in the east occurred at roughly 1800 LST during the wet seasons, but several hours later during the dry seasons. Camberlin et al. (2018) pointed out that the daytime land maximum and nighttime lake maximum is common to many East African lakes. Mahony et al. (2020) showed convergence of wind over the lake at night and the divergence during the day and suggested that the storms formed over land drift over the lake at night, where they become invigorated. Onyango et al. (2020) similarly suggested that the afternoon storms initiated over the land in the northeast propagate westward over the lake. They also found that the afternoon land maximum can be attributed to a high incidence of moderate rainfall while the maximum over the western half of the lake is associated with high rainfall intensity.

Tan et al. (2019) is the only paper to examine the diurnal cycle over Lake Victoria in detail during all four seasons. Based on data from the Integrated Multisatellite Retrievals for Global Precipitation Measurement (GPM) V06 Final Product (IMERG-F), they found that maximum overlake rainfall occurs several hours earlier in March–May than during June–August (the dry season) or during September–November (the secondary rainy season). March–May rainfall exhibited a broad peak between roughly 0000 and 0900 LST.

3. Data and methodology

a. *Overview of the approach*

Most of the Lake Victoria region has a bimodal seasonal distribution of rainfall. The two rainy seasons occur during the two transition seasons. Rainfall is greatest during the "long rains" season, March–May. The secondary rainy season, the "short rains," occurs in October, November, and early December (Nicholson 2015). The characteristics and large-scale forcing of the two rainy seasons are very different (Nicholson 2017). June, July, and August are the driest months. A second dry season occurs in January and February.

The diurnal cycle is examined in the wettest month of each wet season, April and November. It is also examined in the driest month of each dry season, February and July. During February the tropical rainbelt lies to the south of Lake Victoria. In July it lies to the north. By examining these four months, the lake effect is put into the context of highly contrasting large-scale meteorological conditions.

b. *Data*

Nicholson et al. (2021a) compared the performance of four monthly satellite products over Lake Victoria and its catchment: IMERG-F, Precipitation Estimation from Remotely Sensed Information Using Artificial Neural Networks (PERSIANN)-CDR, TRMM 3B43 V7, and Climate Hazards Group Infrared

JOBNAME: JHM 00#00 2021 PAGE: 3 SESS: 8 OUTPUT: Sat Oct 23 07:29:55 2021 Total No. of Pages: 11
/ams/jhm/0/jhmD210083

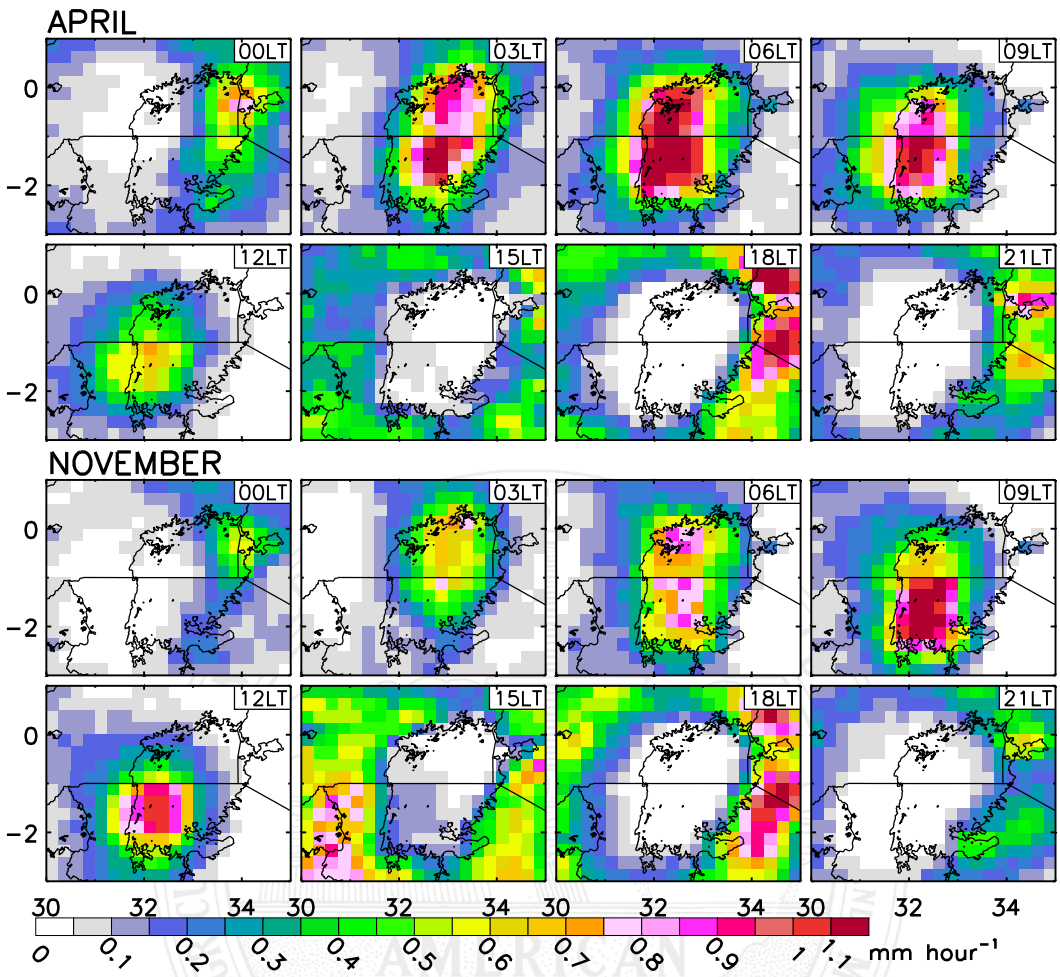

FIG. 2. Mean diurnal cycle of rainfall in April and November.

Precipitation with Station Data (CHIRPS2). TRMM 3B43 V7 provided the best estimates of precipitation. Its daily equivalent, TRMM 3B42 V7, is used in this study.

Based on the performance of TRMM 3B43 V7 in the Lake Victoria region, it is expected that TRMM 3B42 V7 will also perform well here. Support for that assumption comes from Guo and Liu (2016), who found that when TRMM 3B42 values are aggregated to the monthly scale, they provide rainfall estimates extremely close to those of TRMM 3B43. Moreover, several studies have examined the performance of TRMM 3B42 over areas within equatorial Africa and found good agreement with gauge data (e.g., Cattani et al. 2016; Dezfuli et al. 2017; Beighley et al. 2011; Awange et al. 2016; Diem et a. 2014; Asadullah et al. 2008). Haile et al. (2013) showed that TRMM 3B42 did an adequate job in representing the diurnal cycle at island stations in Lake Victoria.

TRMM 3B42 V7 has 6-hourly resolution and will be used in this study. It merges precipitation estimates from several passive microwave sensors with microwave-calibrated infrared-based precipitation estimates and then performs bias adjustment using monthly accumulated rain gauge analysis from the Global Precipitation Climatology Centre (Huffman et al. 2007, 2015; Huffman and Bolvin 2014). It has a spatial resolution of 0.25°, and data are available for 1998–2020.

Counts and locations of MCSs are taken from a dataset of Hartman (2016, 2021), which is based on the GridSat-B1 dataset of NOAA's National Centers for Environmental Information. The MCS dataset is 3-hourly and extends to 35°E. It covers the six rainy season months of March–May, and September–November and runs from 1983 to 2015. MCS occurrence is gridded at 0.5° resolution, and MCS initiations are gridded to 1° resolution.

4. The diurnal cycle of rainfall

a. *The two rainy seasons*

Figure 2 shows monthly rainfall at eight times per day. In April the lake is nearly rainless at 1500 LST while rainfall occurs throughout the surrounding catchment. Rainfall is highest (0.5–1 mm h^{-1}) over the high terrain in the eastern periphery of the basin. Maximum rainfall in that region occurs at 1800 LST, at which time rainfall ceases to the west of the lake. The 1800 LST maximum is somewhat anomalous, because in areas surrounding East African lakes, peak rainfall generally occurs

JOBNAME: JHM 00#00 2021 PAGE: 4 SESS: 8 OUTPUT: Sat Oct 23 07:29:55 2021 Total No. of Pages: 11
/ams/jhm/0/jhmD210083

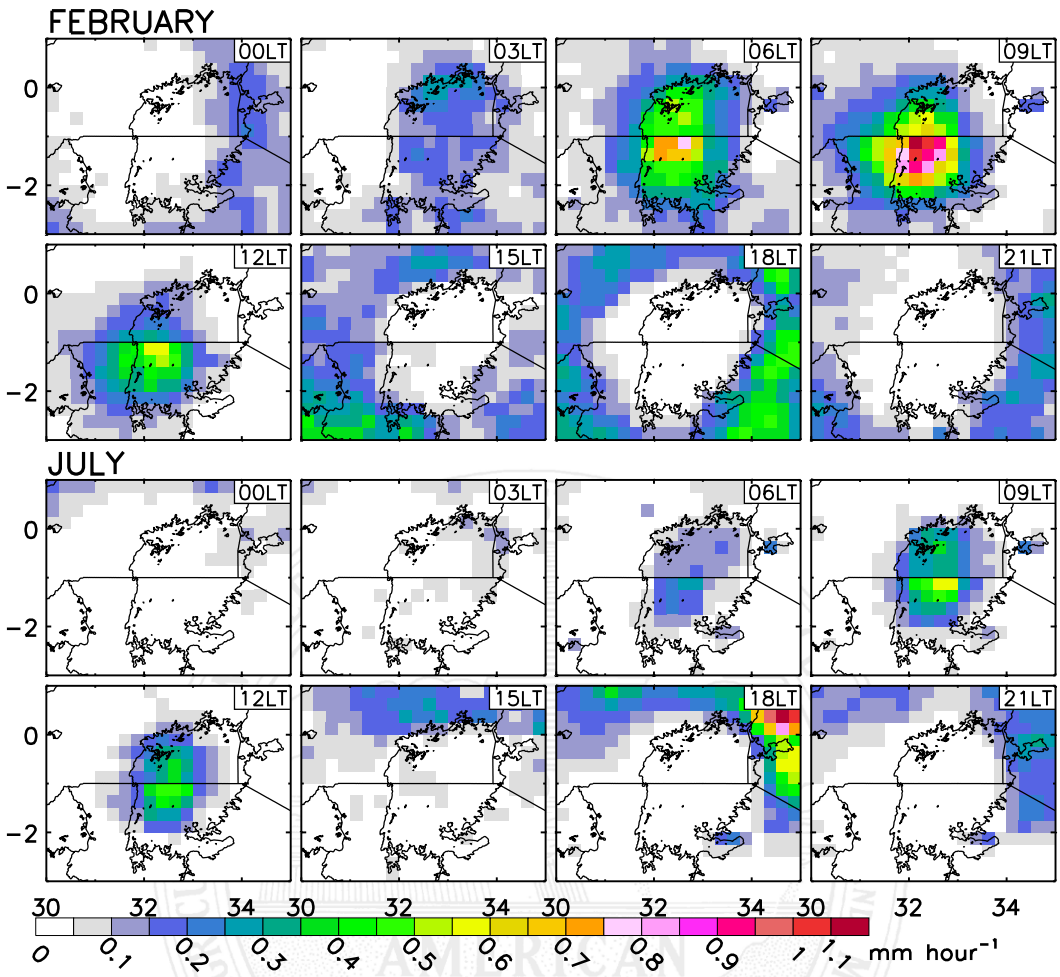

FIG. 3. Mean diurnal cycle of rainfall in February and July.

around 1500 LST (Camberlin et al. 2018). Mahony et al. (2020) suggest the reason for the delayed maximum is stronger lake-breeze effects over Lake Victoria or a positive feedback between the lake breeze and anabatic winds, factors that can increase the intensity and duration of storms. Between 1800 and 0000 LST the rainfall migrates westward toward the center of the lake and conditions become progressively drier to the west of the lake.

By 0300 LST there is an explosive increase in rainfall over the lake with a maximum in its center. Over most of the lake rainfall well exceeds 0.7 mm h^{-1}. Rainfall is decreasing over the high terrain east of the lake. Peak rainfall occurs over the lake at 0600 LST and it is strongest over the western half of the lake, a pattern that continues through 1200 LST. Rainfall exceeds 1 mm h^{-1} over the western half of the lake.

During November the diurnal cycle is exceedingly similar in pattern, but the intensity of rainfall is generally lower. The exception is higher rainfall to the west of the lake at 1500 and 1800 LST. The biggest contrast with April is with the nocturnal overlake rains. As during April rainfall occurs ubiquitously over the lake from 0300 to 1200 LST, but rainfall totals are notably lower and peak rainfall occurs later, at 0900 LST.

b. *The two dry seasons*

The diurnal cycle is considerably different during the dry season months of July and February (Fig. 3). The driest conditions occur during July, when the tropical rainbelt lies well to the north of the lake. The lake is almost completely free of rainfall during five of the time periods, from 1500 to 0300 LST. Rain occurs over most of the lake from 0600 to 1200 LST, with maximum rainfall occurring in the west. Overlake rainfall peaks around 0900 LST. Over the surrounding land there is little rain except during the period 1500–2100 LST. It is confined to areas north and northeast of the lake.

In February lake-effect rains begin earlier than during July, at 0300 LST. Peak rainfall occurs over the lake at 0900 LST, as in July. Clear conditions occur over the lake at only four time periods, running from 1500 to 0000 LST. Over the surrounding land there is considerably more rainfall than during July. From 0300 to 2100 LST it occurs almost throughout the lake catchment. At other times it occurs mainly to the south of the lake, but at 1200 LST nearly the entire catchment is dry.

JOBNAME: JHM 00#00 2021 PAGE: 5 SESS: 8 OUTPUT: Sat Oct 23 07:29:55 2021 Total No. of Pages: 11
/ams/jhm/0/jhmD210083

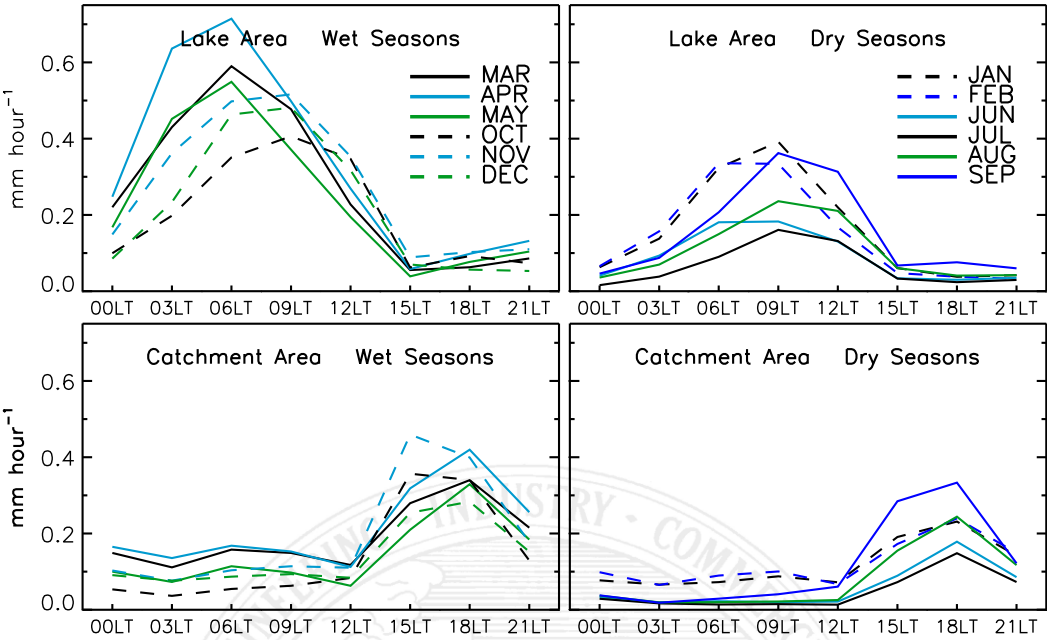

FIG. 4. Mean diurnal cycle over the lake and over the catchment in (left) the wet months and (right) the dry months.

F4 Figure 4 summarizes the diurnal cycle for the lake and catchment during the wet and dry seasons. The dichotomy between nighttime rains over the lake and daytime rains over the catchment is clear in all months. There is also clearly an enhancement of rainfall over the lake, compared to that over the catchment, in all months. The switch from lake to land rainfall occurs between 1200 and 1500 LST in all months.

During the long rains season, rainfall peaks over the lake at 0600 LST and over the catchment at 1800 LST. During the short rains season the nocturnal peak occurs 3 h later and the daytime peak occurs three hours earlier. During the dry seasons the time of peak overlake rainfall varies between 0600 and 0900 LST but catchment rainfall peaks at 1800 LST in all months.

F5 The diurnal cycles in the western and eastern portion of the catchment are compared in Fig. 5. The diurnal cycle is markedly stronger in the east than in the west, especially during the two wet seasons (i.e., the long rains of March–May and the short rains of October–December). Peak rainfall ranges from 0.4 to 0.6 mm h^{-1} in the east, but in the west it is lower than 0.2 mm h^{-1} during May and exceeds 0.4 mm h^{-1} during only two months. In the east there is a pronounced maximum at 1800 LST in all months and little rain occurs between 0300 and 1200 LST. In the west the diurnal cycle of rainfall is bimodal, with a maximum at 1500 LST in all months and a second maximum at 0600 or 0900 LST. In May the nocturnal maximum is greater than the daytime maximum. During the dry season months, rainfall is also much higher in the east than in the west. In all six months the maximum in the east occurs at 1800 LST, and from 0300 to 1200 LST it is almost completely dry. In the west rainfall is bimodal in January and February, but in the remaining months there is a single maximum at 1500 LST. The nocturnal maximum in the west probably reflects the impact of the strong katabatic flow off the eastern highlands.

F6 Figure 6 summarizes the persistence of the timing of peak rainfall. This shows the number of months in which peak rainfall occurs at the same time. There is a clear pattern of high persistence (8–12 months) over the highlands to the east and west of the lake and low persistence over the lake and lowlands to the north, south, and just west of the lake. The strong persistence over the highlands shows the stationary forcing of the mountain–valley winds. The variability over the lake itself and the lowlands probably reflects to some extent the changing contrast between the intensity of that system over the Ruwenzori Mountains to the west and over the East African highlands to the east. Changes in the large-scale winds might also play a role. The timing of peak rainfall is also persistent over the large clusters of islands in the lake, such as the Ssese Islands in the northwest, the Ukerewe Islands in the southeast, Kome Island in the south, and Nabuyongo Island in the central part of the lake. These provide stationary forcing of a more local land–sea breeze system.

c. *Extent of the lake's influence on rainfall*

The results of the analyses of diurnal rainfall give a hint as to the extent of the lake's influence on catchment rainfall. It is seen in Figs. 2 and 3 that the nighttime rains extend to the west and northwest of the lake. A comparison with Fig. 1 suggests that the westward reach of the lake effect rains appears to be constrained by topography. To the east, it is difficult to distinguish between lake-effect rains and the rainfall enhancement by the high topography near the shore. However, the rainfall east of the lake at 0000 and 0300 LST appears to be associated with the afternoon convection, so that the impact of the lake-effect rains to the east appears to be minimal. An impact there is unlikely because the prevailing winds are easterly. Note also the strong persistence of the timing of

JOBNAME: JHM 00#00 2021 PAGE: 6 SESS: 8 OUTPUT: Sat Oct 23 07:29:56 2021 Total No. of Pages: 11
/ams/jhm/0/jhmD210083

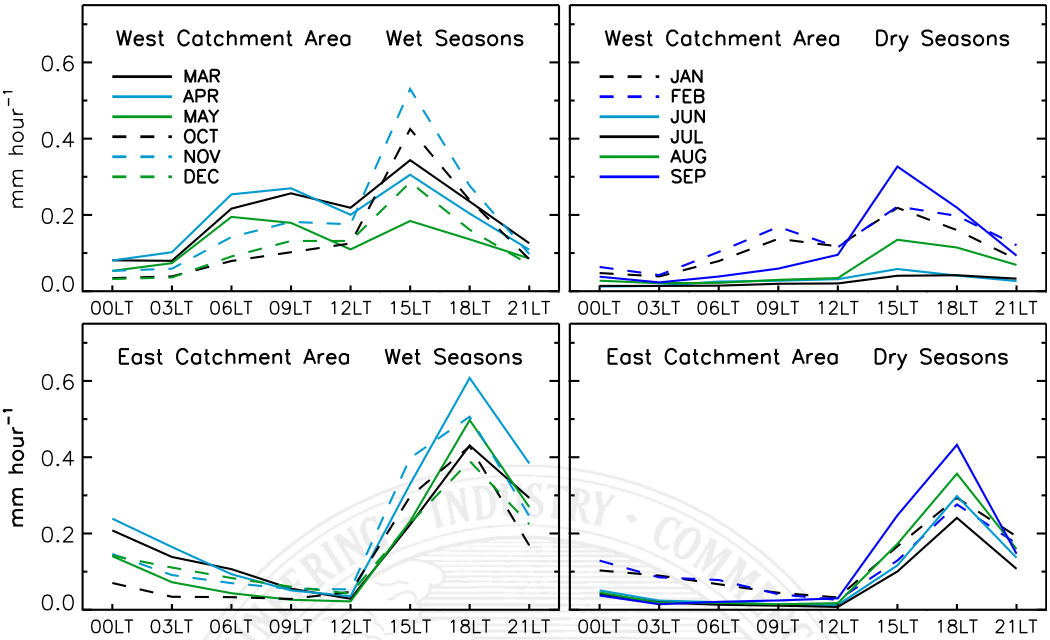

FIG. 5. Mean diurnal cycle over the eastern and western portions of the catchment in (left) the wet months and (right) the dry months.

rainfall in the areas just to the east of the lake (Fig. 6). This suggests that the primary influence there is topography. The region of weak persistence over the lake extends into areas west and slightly north of the lake. Presumably these areas of weak persistence mark the extent of the influence of the lake-effect rains.

5. Mesoscale convective systems

Mesoscale convective systems develop as the merger of individual thunderstorms. Over Lake Victoria thunderstorms develop at night because the lake temperature remains fairly constant while the atmosphere cools substantially, destabilizing the atmosphere over the lake (Flohn and Burkhardt 1985; Datta 1981). The convergence of the land breezes promotes the merger of the individual storms. Initially the MCS grows vertically as it intensifies, producing convective rainfall. As it approaches the tropopause, an anvil develops and spreads out in all directions (Jackson et al. 2009). The result is substantial stratiform rainfall and a spreading of the region receiving rainfall.

F7 Figure 7 shows the diurnal cycle of MCSs over Lake Victoria during April and November. The data represent the total number of MCSs during the period 1983–2015. During both months MCSs occur frequently over the lake but comparatively seldom over most of the land. In April MCSs commonly occur over the lake between 2400 and 1200 LST. At 2400 LST they appear mostly over the eastern half of the lake and at 1200 LST they appear mostly over the western half. Maximum MCS activity over the lake is at 0600 LST. At 0300 LST the maximum count is over the center of the lake but at 0600 and 0900 LST it is in the western portion, where the count (not shown) gets as high as 26.

The picture is very different over the surrounding land. Between 0300 and 1200 LST, when MCSs occur frequently over the lake, they are nearly absent over the land. At 1500 LST a few develop over the highlands to the west of the lake, but at 1800 LST there is a strong surge of MCS activity to the east and northeast of the lake. MCS count increases and the MCSs move westward between 1800 and 0000 LST, and the storms diminish

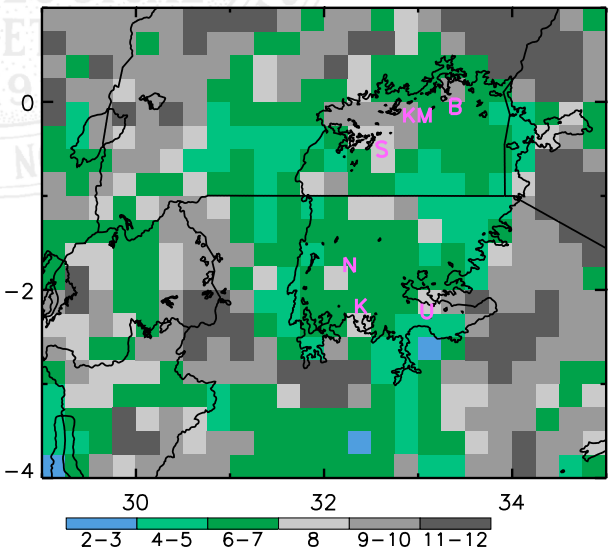

FIG. 6. Persistence of the diurnal cycle of rainfall (see text). Island locations indicated by letters: S = Ssese Islands, U = Ukerewe Islands, N = Nabuyongo Island, KM = Koome Island, K = Kome Island, and B = Buvuma Island.

JOBNAME: JHM 00#00 2021 PAGE: 7 SESS: 8 OUTPUT: Sat Oct 23 07:29:56 2021 Total No. of Pages: 11
/ams/jhm/0/jhmD210083

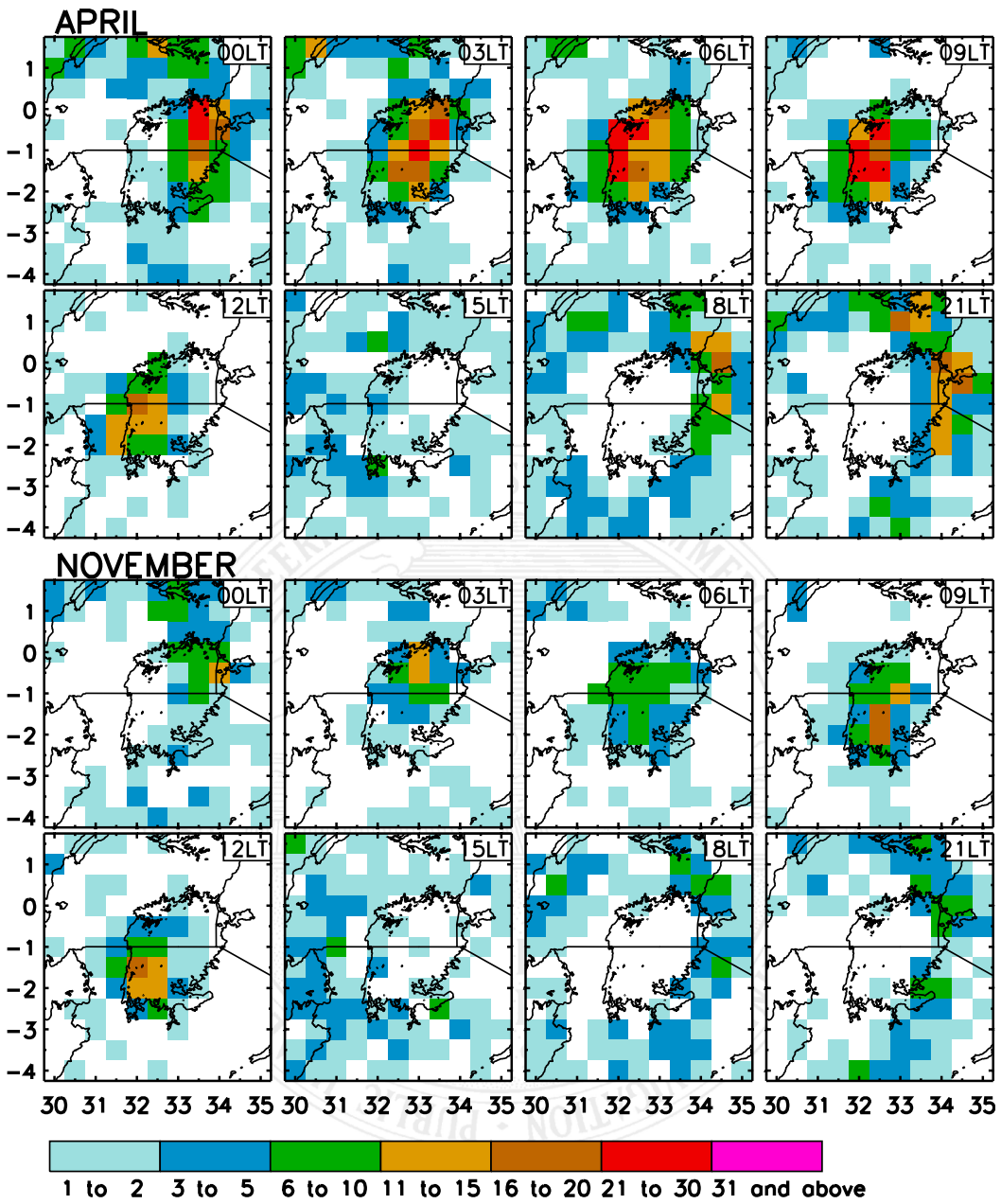

FIG. 7. Mean diurnal cycle of MCS count in April and November.

over the land area to the east of the lake. At 0000 LST the maximum MCS count (not shown) over the eastern fringe of the lake is 18–26. The maximum continues to move westward until 1200 LST. Maximum MCS activity over the lake occurs at 0600 LST and is situated toward the western shore of the lake.

MCS activity is much weaker during November. Over land a few MCSs appear to the west of the lake around 1500 LST and to the east of the lake around 1800 LST. As in April, those move westward over the lake between then and 0000 LST. MCS activity is concentrated over the lake between 0300 and 1200 LST, with greater activity in the west than in the east. The maximum is at around 0900 LST, when 15–17 MCSs occur over the center of the lake.

Mahony et al. (2020) and Onyango et al. (2020) suggest the MCS activity over the lake actually commences over the land, with systems moving westward at night. This idea is tested using MCS initiation counts, shown in Fig. 8 for April and F8 November. In April initiation does begin over the land surrounding the lake around 1500 LST. The count increases at 1800 LST especially to the east of the lake, where the count exceeds 21 in several grid boxes. The eastern maximum does propagate westward over the lake from then until 0000 LST. However, strong initiation is observed over the lake itself at 0300 and 0600 LST. Overlake initiation continues through 1200 LST. The same pattern occurs in November, but with fewer initiations

JOBNAME: JHM 00#00 2021 PAGE: 8 SESS: 8 OUTPUT: Sat Oct 23 07:29:56 2021 Total No. of Pages: 11
/ams/jhm/0/jhmD210083

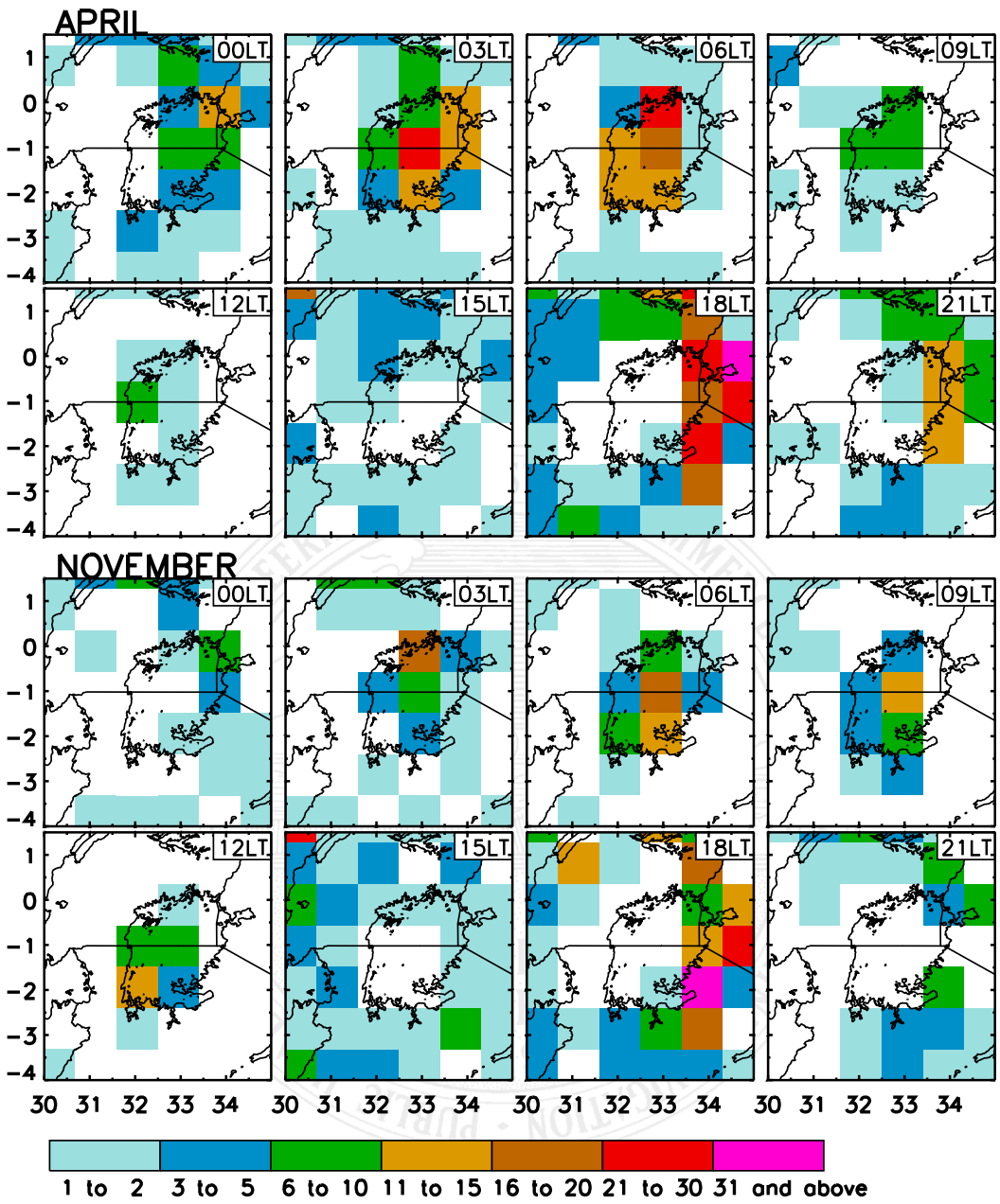

FIG. 8. Mean diurnal cycle of counts of MCS initiation in April and November.

throughout the region. Thus, it seems that there is some propagation of MCSs that initiate over land, but that the majority over the lake initiate in situ.

Nicholson et al. (2021a) explored the relationship between MCS activity and rainfall in the Lake Victoria region on seasonal and interannual time scales. The correlation between monthly rainfall and monthly MCS count was calculated for each of five months over the period 1983–2015. The correlations ranged from 0.77 for October and May to 0.86 for March, suggesting that the interannual annual variability of overlake rainfall is strongly controlled by the number of MCSs that occur. On the other hand, the number of MCSs did not explain the contrasts in overlake rainfall from month to month. However, a comparison of Figs. 2 and 7 suggests that the diurnal cycle of overlake rainfall unsurprisingly appears to mirror the diurnal cycle of MCS activity. This includes the spatial pattern and relative magnitude over the course of the day.

This relationship is highlighted in Fig. 9, which shows the F9 diurnal cycle of rainfall and MCS count over the lake, over the western catchment and over the eastern catchment in April and November. This suggests an overwhelming role of MCS activity in producing the nocturnal rainfall over the lake in April and the strong but weaker role in November. This is consistent with Nesbitt et al. (2006), who found that MCSs

JOBNAME: JHM 00#00 2021 PAGE: 9 SESS: 8 OUTPUT: Sat Oct 23 07:29:56 2021 Total No. of Pages: 11
/ams/jhm/0/jhmD210083

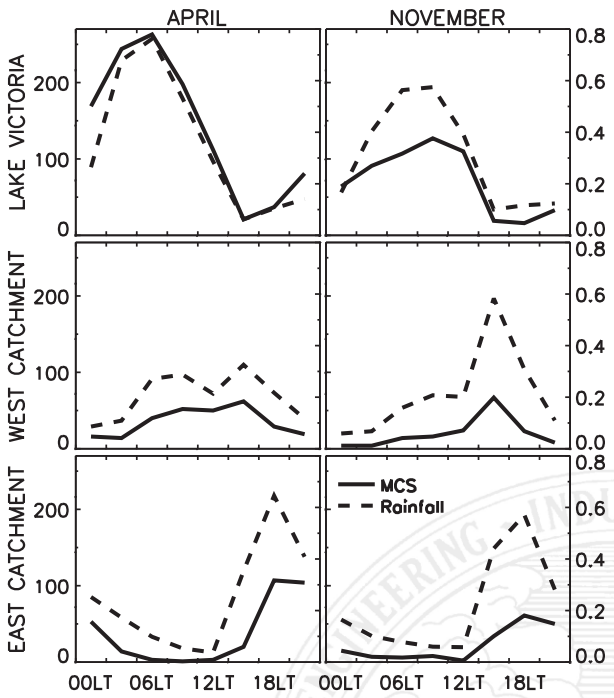

FIG. 9. Average diurnal cycle of MCS activity (right axis scale) over the lake and over the eastern and western portions of the catchment in April and November. Rainfall (left axis scale; mm) is included for comparison.

account for 50%–60% of the rainfall over Lake Victoria, and with Jackson et al. (2009), who concluded they account for 75%–85% of the rainfall during the two rainy seasons.

6. Summary and conclusions

a. Diurnal cycle of rainfall

A major result of this study is to demonstrate that lake-effect rains occur over Lake Victoria not only during the wet seasons but also during both dry seasons. They peak at 0600 LST during the long rains of March–May and at 0900 LST during the short rains of October–December. During the six dry season months they generally peak at 0900 LST as well. Over the catchment they peak at 1800 LST during the long rains and 1500 or 1800 LST during the short rains. During the six dry months the peak over the catchment is at 1800 LST.

During the dry-season months evaluated, July and February, overlake rainfall was more limited in spatial extent and duration and smaller in magnitude than during the two wet-season months, April and November. The diurnal cycle was similar in April and November, but rainfall was overall lower in November. In these months, rainfall occurred over most or all of the lake between 0000 and 1200 LST. At 1500 LST some rainfall was evident in the southwest and rainfall was evident in the east at the remaining times. In contrast, during February rainfall occurred over most or all of the lake from 0300 to 1200 LST and was extremely limited spatially or absent at other times. In July lake-effect rains were apparent only between 0600 and 1200 LST and did not extend over the entire lake.

There is a clear dichotomy between overlake rainfall and catchment rainfall. Overlake rainfall peaks during the night and early morning and is much stronger than catchment rainfall, which peaks during the afternoon and early evening. In general, it is dry over the lake when rainfall occurs over the catchment and, conversely, dry over the catchment when rainfall occurs over the lake. The transition between lake and catchment rainfall occurs in all months between 1200 and 1500 LST. Rainfall is higher over the eastern part of the catchment than over the western, likely a consequence of topographic contrasts between the East African highlands in the east and the Ruwenzori Mountains in the west.

Although the diurnal cycle over Lake Victoria is clear and robust, it is not representative of other East African lakes (Camberlin et al. 2018). A similar pattern is evident over the two very large lakes, Tanganyika and Malawi, but the daytime suppression is weaker than over Lake Victoria (Nicholson et al. 2021b). The smaller lakes enhance rainfall over the lake itself AU2 but tend to have a bimodal maximum in the diurnal cycle. The nocturnal maximum appears to be lake-effect rains while the afternoon maximum appears to be due to advection of systems developed over land. Further research is needed to better understand the contrasts in the various lakes.

b. Association with MCSs

The MCS dataset used only includes wet season months, so only April and November are considered. MCS activity is weaker in November and may help account for the weaker lake-effect rains in November. MCS initiation generally begins over the catchment around 1500 LST and increases at 1800 LST. There appears to be some propagation of these systems westward over the lake. However, MCS initiation over the lake itself clearly begins around 0300 LST and continues until 1200 LST. While some MCSs originate over the highlands to the east of the lake, most originate in situ over the lake. Maximum MCS activity over the lake occurs at 0600 LST and is associated with the systems that initiate in situ.

Acknowledgments. SEN and DK were supported by two grants from the National Science Foundation, GEO/ATM 1854511 and EAR 1850661. The work of ATH was supported by NSF Grant AGS 1535439.

Data availability statement. The datasets utilized are in the public domain. The exception is the MCS dataset. It can be obtained by contacting the first author.

REFERENCES

Akurut, M., P. Willems, and C. B. Niwagaba, 2014: Potential impacts of climate change on precipitation over Lake Victoria, East Africa, in the 21st Century. *Water*, **6**, 2634–2659, https://doi.org/10.3390/w6092634.

Asadullah, A., N. McIntyre, and M. Kigobe, 2008: Evaluation of five satellite products for estimation of rainfall over Uganda. *Hydrol. Sci. J.*, **53**, 1137–1150, https://doi.org/10.1623/hysj.53.6.1137.

Awange, J. L., V. G. Ferreira, E. Forootan, K. Khandu, S. A. Andam-Akorful, N. O. Agutu, and X. F. He, 2016: Uncertainties in

remotely sensed precipitation data over Africa. *Int. J. Climatol.*, **36**, 303–323, https://doi.org/10.1002/joc.4346.

Ba, M. B., and S. E. Nicholson, 1998: Analysis of convective activity and its relationship to the rainfall over the Rift Valley lakes of East Africa during 1983–90 using Meteosat infrared channel. *J. Appl. Meteor.*, **37**, 1250–1264, https://doi.org/10.1175/1520-0450(1998)037<1250:AOCAAI>2.0.CO;2.

Bargman, D. J., Ed., 1960: *Tropical Meteorology in Africa*. Munitalp Foundation, 446 pp.

Bedka, K., J. Brunner, R. Dworak, W. Feltz, J. Otkin, and T. Greenwald, 2010: Objective satellite-based detection of overshooting tops using infrared window channel brightness temperature gradients. *J. Appl. Meteor. Climatol.*, **49**, 181–202, https://doi.org/10.1175/2009JAMC2286.1.

Beighley, R. E., and Coauthors, 2011: Comparing satellite derived precipitation datasets using the Hillslope River Routing (HRR) model in the Congo River basin. *Hydrol. Processes*, **25**, 3216–3229, https://doi.org/10.1002/hyp.8045.

Berson, A., 1910: *Bericht über die aerologische Expedition des königlichen aeronautischen Observatoriums nach Ostafrika im Jahre 1908*. Vieweg, 119 pp.

Camberlin, P., W. Gitau, O. Planchon, V. Dubreuil, B. M. Funatsu, and N. Philippon, 2018: Major role of water bodies on diurnal precipitation regimes in Eastern Africa. *Int. J. Climatol.*, **38**, 613–629, https://doi.org/10.1002/joc.5197.

Cattani, E., A. Merino, and V. Levizzani, 2016: Evaluation of monthly satellite-derived precipitation products over East Africa. *J. Hydrometeor.*, **17**, 2555–2573, https://doi.org/10.1175/JHM-D-15-0042.1.

Chamberlain, J. M., C. L. Bain, D. F. A. Boyd, K. McCourt, T. Butcher, and S. Palmer, 2014: Forecasting storms over Lake Victoria using a high resolution model. *Meteor. Appl.*, **21**, 419–430, https://doi.org/10.1002/met.1403.

Datta, R. R., 1981: Certain aspects of monsoonal precipitation dynamics over Lake Victoria. *Monsoon Dynamics*, J. Lighthill and R. P. Pearce, Eds., Cambridge University Press, 333–349.

Dezfuli, A. K., C. M. Ichoku, G. J. Huffman, K. I. Mohr, J. S. Selker, N. van de Giesen, R. Hochreutener, and F. O. Annor, 2017: Validation of IMERG precipitation in Africa. *J. Hydrometeor.*, **18**, 2817–2825, https://doi.org/10.1175/JHM-D-17-0139.1.

di Baldassarre, G., and Coauthors, 2011: Future hydrology and climate in the River Nile basin: A review. *Hydrol. Sci. J.*, **56**, 199–211, https://doi.org/10.1080/02626667.2011.557378.

Diem, J. E., J. Hartter, S. J. Ryan, and M. W. Palace, 2014: Validation of satellite rainfall products for western Uganda. *J. Hydrometeor.*, **15**, 2030–2038, https://doi.org/10.1175/JHM-D-13-0193.1.

Flohn, H., 1983: Das Katastrophenregen 1961/62 und die Wasserbilanz des Viktoria-See-Gebietes. Wissenschaftliche Berichte des Meteorologischen Instituts der Universität Karlsruhe 4, 17–34.

——, and K. Fraedrich, 1966: Tagesperiodische zirkulation und niederschlagsverteilung am Victoria-See (Ostafrika). *Meteor. Rundsch.*, **6**, 157–165.

——, and T. Burkhardt, 1985: Nile runoff at Aswan and Lake Victoria; An example of a discontinuous climate time series. *Z. Gletschkd. Glazialgeol.*, **21**, 125–130.

Fraedrich, K., 1968: Das Land- und Seewindsystem des Victoria-Sees nach aerologischen Daten. *Arch. Meteor. Geophys. Bioklimatol.*, **17**, 186–206, https://doi.org/10.1007/BF02247084.

——, 1971: Model einer lokalen atmosphaerischen Zirkulation mit Anwending auf den Victoria-See. *Beitr. Phys. Atmos.*, **44**, 95–114.

——, 1972: A simple climatological model of the dynamics and energetics of the nocturnal circulation at Lake Victoria. *Quart. J. Roy. Meteor. Soc.*, **98**, 322–335, https://doi.org/10.1002/qj.49709841606.

Guo, R., and Y. Liu, 2016: Evaluation of satellite precipitation products with rain gauge data at different scales: Implications for hydrological applications. *Water*, **8**, 281–300, https://doi.org/10.3390/w8070281.

Haile, A. T., E. Habib, M. Elsaadani, and T. Rientjes, 2013: Inter-comparison of satellite rainfall products for representing rainfall diurnal cycle over the Nile basin. *Int. J. Appl. Earth Obs. Geoinf.*, **21**, 230–240, https://doi.org/10.1016/j.jag.2012.08.012.

Hartman, A. T., 2016: Tracking and analysis of mesoscale convective systems over central equatorial Africa. M.S. thesis, Dept. of Earth, Ocean, and Atmospheric Science, Florida State University, 58 pp., http://purl.flvc.org/fsu/fd/FSU_FA2016_Hartman_fsu_0071N_13642.

——, 2021: Tracking mesoscale convective systems in central equatorial Africa. *Int. J. Climatol.*, **41**, 469–482, https://doi.org/10.1002/joc.6632.

Holle, R. L., and M. J. Murphy, 2017: Lightning over three tropical lakes and the Strait of Malacca: Exploratory analyses. *Mon. Wea. Rev.*, **145**, 4559–4573, https://doi.org/10.1175/MWR-D-17-0010.1.

Huffman, G. J., and D. T. Bolvin, 2014: TRMM and other data precipitation data set documentation. NASA TRMM Doc., 42 pp., ftp://precip.gsfc.nasa.gov/pub/trmmdocs/3B42_3B43_doc.pdf.

——, and Coauthors, 2007: The TRMM multi-satellite precipitation analysis: Quasi-global, multi-year, combined-sensor precipitation estimates at finer scale. *J. Hydrometeor.*, **8**, 38–55, https://doi.org/10.1175/JHM560.1.

——, D. T. Bolvin, and E. J. Nelkin, 2015: Day 1 IMERG final run release notes. NASA Doc., 9 pp., http://pmm.nasa.gov/sites/default/files/document_files/IMERG_FinalRun_Day1_release_notes.pdf.

Jackson, B., S. E. Nicholson, and D. Klotter, 2009: Mesoscale convective systems over western equatorial Africa and their relationship to large-scale circulation. *Mon. Wea. Rev.*, **137**, 1272–1294, https://doi.org/10.1175/2008MWR2525.1.

Kayiranga, T., 1991: Observation of convective activity from satellite data over the Lake Victoria region in April 1985 (in French). *Veille Climatique Satellitaire*, **37**, 44–55.

Kizza, M., I. Westerberg, A. Rodhe, and H. K. Ntale, 2012: Estimating areal rainfall over Lake Victoria and its basin using ground-based and satellite data. *J. Hydrol.*, **464–465**, 401–411, https://doi.org/10.1016/j.jhydrol.2012.07.024.

Lumb, F. E., 1970: Topographic influences on thunderstorm activity near Lake Victoria. *Weather*, **25**, 404–410, https://doi.org/10.1002/j.1477-8696.1970.tb04129.x.

Mahony, J., E. Dyer, and R. Washington, 2020: The precipitation patterns and atmospheric dynamics of the Serengeti National Park. *Int. J. Climatol.*, **41**, E2051–E2072, https://doi.org/10.1002/joc.6831.

Nesbitt, S. W., R. Cifelli, and S. A. Rutledge, 2006: Storm morphology and rainfall characteristics of TRMM precipitation features. *Mon. Wea. Rev.*, **134**, 2702–2721, https://doi.org/10.1175/MWR3200.1.

Nicholson, S. E., 2015: Long-term variability of the East African 'short rains' and its links to large-scale factors. *Int. J. Climatol.*, **35**, 3979–3990, https://doi.org/10.1002/joc.4259.

——, 2017: Climate and climatic variability of rainfall over eastern Africa. *Rev. Geophys.*, **55**, 590–635, https://doi.org/10.1002/2016RG000544.

——, and X. G. Yin, 2002: Mesoscale patterns of rainfall, cloudiness and evaporation over the Great Lakes of East Africa.

JOBNAME: JHM 00#00 2021 PAGE: 11 SESS: 8 OUTPUT: Sat Oct 23 07:29:57 2021 Total No. of Pages: 11
/ams/jhm/0/jhmD210083

The East African Great Lakes: Limnology, Palaeolimnology and Biodiversity, E. O. Odada and D. Olago, Eds., Springer, 93–119.

——, D. Klotter, and A. T. Hartman, 2021a: Lake-effect rains over Lake Victoria and their association with mesoscale convective systems. *J. Hydrometeor.*, **22**, 1353–1368, https://doi.org/10.1175/JHM-D-20-0244.1.

——, A. T. Hartman, and D. A. Klotter, 2021b: On the diurnal cycle of rainfall and convection over Lake Victoria and its catchment. Part II: Meteorological factors in the diurnal and seasonal cycles. *J. Hydrometeor.*, https://doi.org/10.1175/JHM-D-21-0085.1, in press.

Onyango, A. O., H. Xu, and Z. Lin, 2020: Diurnal cycle of rainfall over Lake Victoria Basin during the long-rain season based on TRMM satellite estimate. *Int. J. Climatol.*, **40**, 4622–4637, https://doi.org/10.1002/joc.6479.

Sene, K. J., 2000: Theoretical estimates for the influence of Lake Victoria on flows in the upper White Nile. *Hydrol. Sci. J.*, **45**, 125–145, https://doi.org/10.1080/02626660009492310.

Tan, J., G. J. Huffman, D. T. Bolvin, and E. J. Nelkin, 2019: Diurnal cycle of IMERG V06 precipitation. *Geophys. Res. Lett.*, **46**, 13 584–13 592, https://doi.org/10.1029/2019GL085395.

Thiery, W., E. L. Davin, H. J. Panitz, M. Demuere, S. Lhermitte, and N. van Lipzig, 2015: The impact of the African Great Lakes on regional climate. *J. Climate*, **28**, 4061–4085, https://doi.org/10.1175/JCLI-D-14-00565.1.

——, ——, S. I. Seneviratne, K. Bedka, S. Lhermitte, and N. P. M. van Lipzig, 2016: Hazardous thunderstorm intensification over Lake Victoria. *Nat. Commun.*, **7**, 12 786, https://doi.org/10.1038/ncomms12786.

Virts, K. S., and S. J. Goodman, 2020: Prolific lightning and thunderstorm initiation over the Lake Victoria Basin in East Africa. *Mon. Wea. Rev.*, **148**, 1971–1985, https://doi.org/10.1175/MWR-D-19-0260.1.

Yin, X., S. E. Nicholson, and M. B. Ba, 2000: On the diurnal cycle of cloudiness over Lake Victoria and its influence on evaporation from the lake. *Hydrol. Sci. J.*, **45**, 407–424, https://doi.org/10.1080/02626660009492338.

Yin, X. G., and S. E. Nicholson, 1998: The water balance of Lake Victoria. *Hydrol. Sci. J.*, **43**, 789–811, https://doi.org/10.1080/02626669809492173.

——, and ——, 2002: Interpreting annual rainfall from the levels of Lake Victoria. *J. Hydrometeor.*, **3**, 406–416, https://doi.org/10.1175/1525-7541(2002)003<0406:IARFTL>2.0.CO;2.